Partially coherent ambiguity functions for depth-variant point spread function design

R. Horstmeyer[1], **S.B. Oh**[2], **O. Gupta**[1], and **R. Raskar**[1]

[1]MIT Media Lab, USA
[2]MIT Department of Mechanical Engineering, USA

Abstract— The ambiguity function (AF) provides a convenient way to model how a camera with a modified aperture responds to defocus. We use the AF to design an optimal aperture distribution, which creates a depth-variant point spread function (PSF) from a sparse set of desired intensity patterns at different focal depths. Prior knowledge of the coherence state of the light is used to constrain the optimization in the mutual intensity domain. We use an assumption of spatially coherent light to design a fixed-pattern aperture mask. The concept of a dynamic aperture mask that displays several aperture patterns during one image exposure is also suggested, which is modeled under an assumption of partially coherent light. Parallels are drawn between the optimal aperture functions for this dynamic mask and the eigenmodes of a coherent mode decomposition. We demonstrate how the space of design for a 3D intensity distribution of light using partially coherent assumptions is less constrained than under coherent light assumptions.

1. INTRODUCTION

Modifying a conventional camera with an aperture mask and a matched post-processing step can extend imaging capabilities into a variety of domains, potentially facilitating depth estimation, object tracking, extended depth-of-field or even super-resolution. Recently, an iterative "mode-selective" method of designing aperture masks using a sparse set of desired PSF intensity distributions at different planes of focus was presented [1]. The set of PSFs is used to generate a desired ambiguity function (AF), which can completely represent a camera's response to defocus. The mode-selection algorithm converges to a valid AF solution that minimizes the mean-squared error between its associated PSFs and the input set of desired PSFs. This AF solution directly yields the optimal aperture mask amplitude and phase distribution to place at the camera pupil plane. If the set of desired PSFs are not physically realizable from a thin mask (i.e., do not obey the constraints of propagation), the algorithm converges to a nearby solution that is realizable.

The mode-selection algorithm is among a class of techniques, including phase retrieval [2], phase space tomography [3] and transport-of-intensity [4], which determine the amplitude and phase of a wavefront from multiple intensity distributions at planes along the direction of propagation. Unlike other methods, mode-selection applies a global constraint to the solution set in the mutual intensity domain, based on a singular value decomposition (SVD). In [1], a spatially coherent mutual intensity function J_c is used as a constraint to determine a fixed aperture mask pattern. Following, we present a method to extend the mode–selection algorithm to operate with a dynamic aperture mask, which can display a set of M amplitude and phase distributions over the course of one image exposure. Each mask in the set is determined from a unique orthogonal mode of the coherent mode decomposition of J. These modes can be found from the M largest singular values of the SVD of J. Since the desired AF is comprised of more than one orthogonal mutual intensity mode, it is equivalent to the optimizing the AF and J of a partially coherent system.

2. MODE-SELECTION FOR APERTURE MASK DESIGN

It is well known that the AF can model the response of an imaging system as a polar display of its optical transfer functions (OTFs) at different planes of defocus [5]. Specifically, if we consider the simplified 1D imaging setup in Fig. (1) with a 1D plane wave $U(x)$ at aperture coordinate x, then the 2D AF of the setup is given by,

$$AF(x', u) = \int U\left(x + \frac{x'}{2}\right) U^*\left(x - \frac{x'}{2}\right) e^{-2\pi i x u} dx \tag{1}$$

where x and x' are the space and spatial frequency coordinates at the pupil plane, respectively, u is a second parameter proportional to defocus, and the asterisk represents complex conjugation. The 1D PSF of the

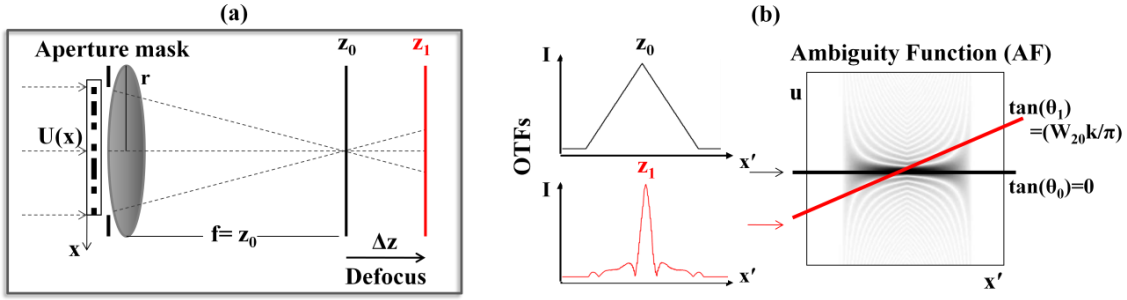

Figure 1: (a) Simplified 1D diagram of a camera setup with an aperture mask in the pupil plane. The mask will generate different OTFs at different planes of defocus. (b) The OTFs of an open aperture in focus (at z_0) and defocused (at z_1) are given as slices of the AF from Eq 2. Note that although the AF is complex, diagrams will show its absolute value.

camera at different planes of defocus along z can be transformed into a 1D OTF $H(x', \Delta z)$ through a Fourier transform relationship [6]. Each OTF can be simply represented as a slice through the camera's AF:

$$H(x', W_{20}) = A(x', x' W_{20} k/\pi) \tag{2}$$

Here, W_{20} is a defocus coefficient related to the defocus distance Δz with $W_{20} = r^2 \Delta z/(2f^2 + 2f\Delta z)$, k is the wavenumber, r is the aperture radius and f is its focal length. Besides this useful connection to the OTF, the mutual intensity function of the wavefront $U(x)$ is also obtainable from the AF through an inverse Fourier transform and coordinate transformation to center-difference coordinates x_1 and x_2:

$$U(x_1)U^*(x_2) = U(x + \frac{x'}{2})U^*(x - \frac{x'}{2}) = \int A(x', u) e^{-2\pi i x u} du \tag{3}$$

The wavefront itself can be recovered from the original AF up to a constant phase factor by setting $x_2 = x - x'/2 = 0$ in Eq. 3. The above equations are implemented in an iterative algorithm in [1] to create a physically valid AF and associated aperture mask distribution from a sparse set of desired intensity inputs. Please refer to Fig. 2. Specifically, a desired set of OTFs (directly generated from a desired PSF set) is used to populate an initial AF estimate at slices given by Eq. 2. After a linear interpolation to fill in zeros, the mutual intensity of the estimated AF, $J'(x_1, x_2)$, is obtained with Eq. 3. After application of a constraint, which will be discussed shortly, a more accurate mutual intensity function $J_{opt}(x_1, x_2)$ is created. J_{opt} is transformed back into the AF domain through application of Eq. 1, where the desired OTF set again populates the AF at slices given by Eq. 2. This procedure iterates until a threshold error value, at which point Eq. 3 is applied with x_2 set to 0 to determine the optimal amplitude and phase distribution to use as an aperture mask. The iterative replacement of OTF values is quite similar to the iterative replacement of amplitude values in the well-known phase retrieval methods of Fienup [2], but instead replaces values and constrains the entire system each iteration instead of cycling through one depth plane at a time.

3. MODE-SELECTION AND COHERENT MODES

3.1. Fixed Aperture Mask uses a Spatially Coherent Constraint

The constraint applied to convert an approximate AF to a physically valid function is based on the required coherence state of the theoretical camera setup in Fig. 1. For a PSF measurement by a camera with a fixed aperture mask, a spatially coherent mutual intensity function is assumed, since $U(x)$ originates from a spatially coherent point source. Thus, $J'(x_1, x_2)$ must be converted to a function $J_c(x_1, x_2)$ that is fully separable, i.e. $J_c(x_1, x_2) = U(x_1)U^*(x_2)$. Taking a linear algebra viewpoint, as with any 2D matrix, the NxN discrete mutual intensity matrix estimate J' can be represented with an SVD:

$$J'(x_1, x_2) = S\Lambda V^T = \sum_{i=1}^{N} s_i \lambda_i v_i \tag{4}$$

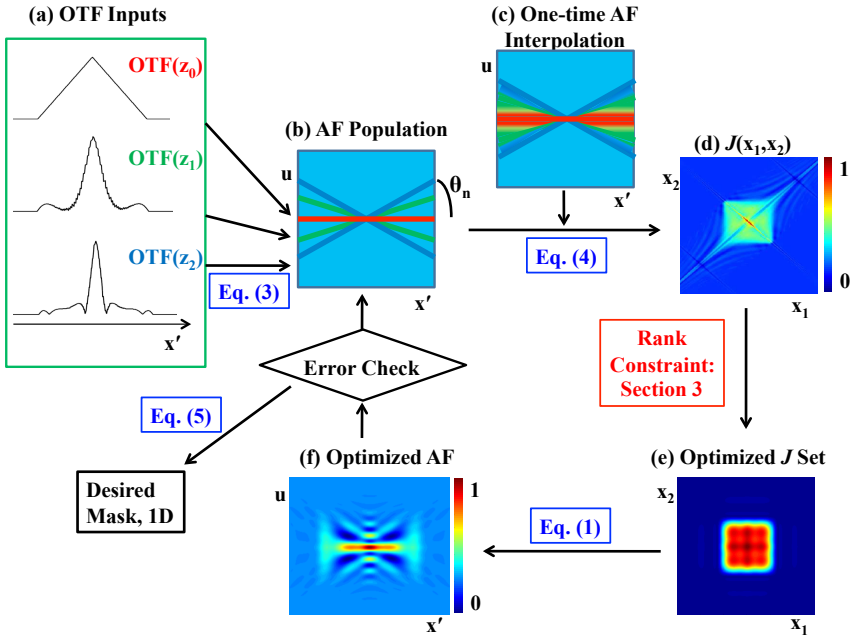

Figure 2: A schematic diagram of the mode-selection algorithm operating in 1D. (a) A set of n desired OTFs (here $n = 3$ for an open aperture), which are determined from desired PSF responses, are used as input. (b) Each OTF populates a slice of the AF, then filled in with a one-time linear interpolation (c). (d) The mutual intensity (J) can be constrained by taking its singular value decomposition shown in (e). (f) An optimized AF is now obtained, which is re-populated with the desired OTF values in (a) along the specific slices in (b). Iteration is stopped at a specified error value, and Eq. (3) is then used to invert the AF into the optimal 1D aperture mask.

Furthermore, from [7], we know that an optimized discrete *coherent* mutual intensity J_c must fulfill a rank-1 condition. A good rank-1 approximation is given by the first singular value of the SVD in Eq. 4,

$$J_c(x_1, x_2) = \sum_{i=1}^{1} s_i \lambda_i v_i = \lambda_1 \mid s_1 \rangle \langle v_1 \mid . \tag{5}$$

In other words, to fulfill the coherence constraint implicit in a PSF measurement, we can represent J_c as the outer-product between the first column of S (s_1), and the first row of V (v_1). Since a spatially coherent wave is composed of a single mutual intensity mode, all singular values besides λ_1 are 0. This constraint reduces our redundant 2D phase space representation to the 2 1D vectors s_1 and v_1, which are equal if J is positive semi-definite.

3.2. Applying a Partially Coherent Constraint

The choice to use the SVD of $J(x_1, x_2)$ to obtain a coherent mutual intensity is based upon the well-known coherent mode decomposition [8], which states that the mutual intensity of a source of any coherence state can be represented as a summation of N mutually orthogonal coherent modes. The SVD provides just such a decomposition into mutually orthogonal components, each with a specific weight λ_i, for any complex 2D matrix. Thus, we can extend the coherence decomposition in Eq. 4 to a given degree of partial coherence by adding up the first M singular values of the SVD of $J(x_1, x_2)$, where $M < N$:

$$J_{pc}(x_1, x_2) = \sum_{i=1}^{M} s_i \lambda_i v_i = \sum_{i=1}^{M} U_i(x_1) U_i^*(x_2) \tag{6}$$

From the Eckart-Young Theorem, it is clear $J_{pc}(x_1, x_2)$ is an optimal approximation of $J(x_1, x_2)$, since J_{pc} is the rank-M approximation of J with minimized Euclidean error [9]. Furthermore, since each mode is orthogonal, $J_{pc}(x_1, x_2)$ consists of a sum of M unique, coherent mutual intensities. Implementing this new constraint in the mode-selection process, $J_{pc}(x_1, x_2)$ will be transformed each iteration into an AF of

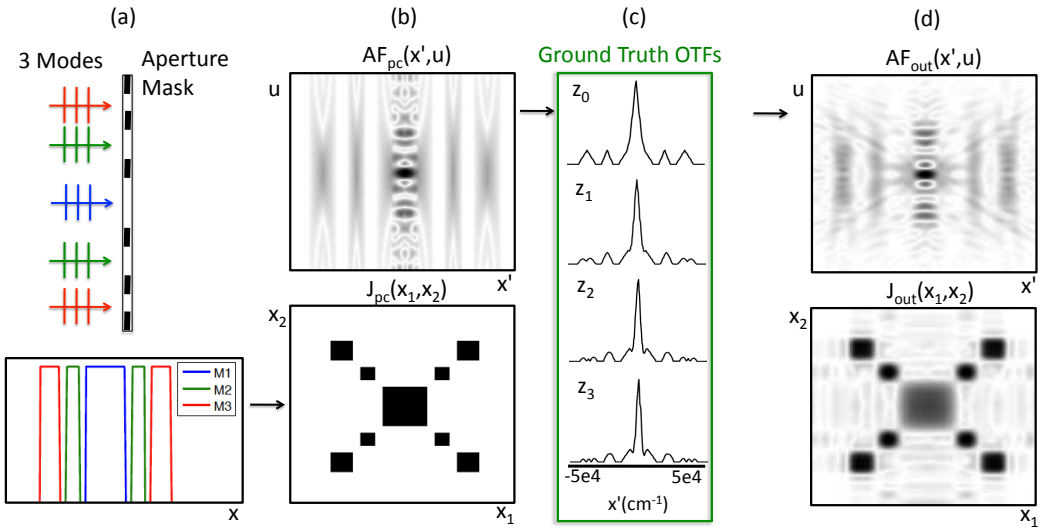

Figure 3: Demonstration of the mode-selection algorithm applied to a known partially coherent input. (a) 3 mutually incoherent plane waves strike an aperture at different locations, creating 3 orthogonal coherent modes. (b) The partially coherent AF_{pc} and mutual intensity J_{pc} (rank 3) for this scenario (maximum is black). (c) 4 OTF slices from AF_{pc}, corresponding to 4 different defocus planes along z, are used as algorithm input. (d) The optimized AF_{out} and J_{out}.

a partially coherent source,

$$AF_{pc}(x',u) = \int J_{pc}(x+\frac{x'}{2}, x-\frac{x'}{2})e^{2\pi i x u}dx = \sum_{i=1}^{M} \lambda_i AF_i(x',u) \tag{7}$$

Here we also express AF_{pc} as a summation over coherent, orthogonal AF_i's, which follows from a similar property of the AFs Fourier dual, the Wigner distribution [10]. Each AF_i obeys Eq. 1 for an orthogonal mode $U_i(x)$. Eq. 7 demonstrates that optimizing for a partially coherent AF is equivalent to simultaneously optimizing M coherent, mutually orthogonal As that must be added to create a desired set of input PSF intensities. These M coherent AFs will provide a *set* of M aperture masks at the algorithm's output, each weighted by its associated singular value λ_i. This summation of AFs to achieve a desired response is directly connected to the longstanding problem of OTF synthesis, studied earlier by Marechal [6]. As with synthesizing OTFs, one way to implement the summation in Eq. 7 is to multiplex each coherent mode over time, which has previously been proposed to simulate partially coherent illumination [11]. Specifically, the fixed aperture mask in Fig. 1(a) can be replaced with a dynamic screen, like a spatial light modulator (SLM), which can display the aperture mask associated with each coherent mode for a finite amount of time over the duration of one image exposure. The length of time each mode is displayed will be proportional to its singular value λ_i. We will now demonstrate that multiple aperture masks can offer additional flexibility in creating a desired depth-dependent PSF as compared to a single aperture mask.

4. PARTIALLY COHERENT AMBIGUITY FUNCTIONS FOR DESIGN

To incorporate partial coherence effects into the algorithm described in Section 2, only the rank constraint connecting Fig. 2(d) and Fig. 2(e) must be modified with Eq. 6. For a given input set of PSFs and a desired number of coherent modes M, this simple change will allow mode-selection to find M optimal weighted aperture mask functions. In most cases, these M aperture functions will lead to a depth-dependent PSF that is a closer match to the desired input as compared with the PSF created by a single aperture function.

First, as a demonstration of the mode selection algorithms ability to accurately converge, performance is tested for a set of ground-truth OTFs that are known to obey the constraints of partially coherent propagation. This is equivalent to testing mode-selection's ability to recreate an entire partially coherent AF from a few OTF inputs. Here, each OTF will be a sum of the OTFs produced by a set of known aperture masks at a given defocus plane. Fig. 3(b) displays an example partially coherent J_{pc} and AF_{pc} used to generate 4 input OTFs: in-focus, at $W_{20} = .5\lambda$, at $W_{20} = \lambda$ and at $W_{20} = 1.5\lambda$. For a 10mm mask and a lens with 50mm focal length, this corresponds roughly to 0.2mm, 0.4mm and 0.6mm of sensor defocus, respectively.

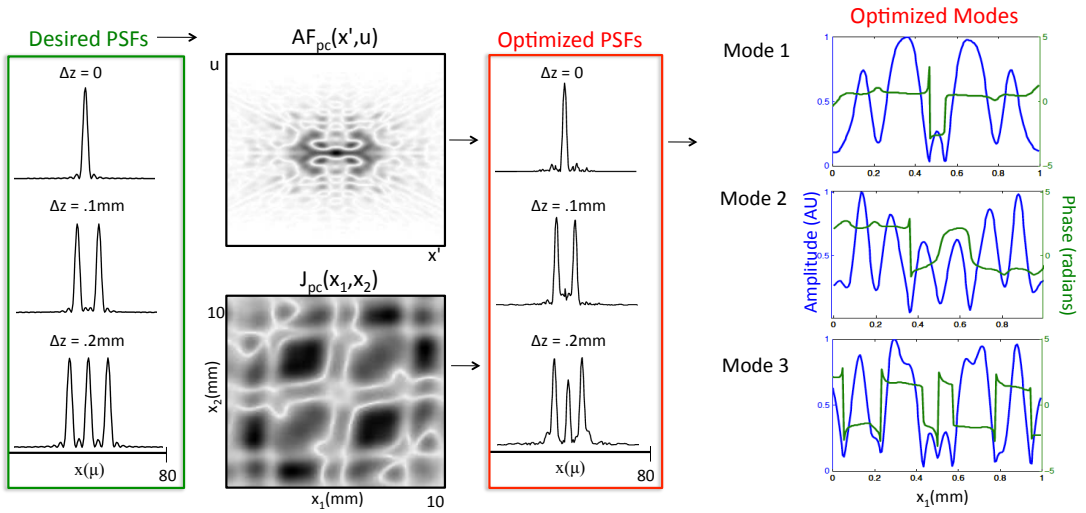

Figure 4: The mode-selection algorithm applied to determining an optimal aperture mask set from a desired depth–dependent PSF (left), with $M = 3$. The algorithm yields 3 1D mask functions (right), each for 1 mode of J.

A faithful reproduction is achieved after 50 algorithm iterations. The performance metric of mean-squared error (MSE) from desired OTFs is $8\text{x}10^{-4}$, which is on the same order as coherent-only operation. MSE is defined as the normalized squared difference between model input (i.e., ground truth OTFs) and output. Errors can be attributed to the limited maximum angle of the OTF slices (similar to the limited-angle problem in tomographic reconstruction), as well as a large amount of rapid changes from 3 overlapping central AF cross-terms in this particular example.

Second, the partially coherent rank-selection algorithm is applied to the problem of designing a desired PSF response (Fig. 4). Specifically, a set of desired input PSF intensities that may not obey the constraints of propagation are used as input (i.e., one point turning into two and then three points at three defocus planes). The algorithm iterates to find an optimal rank-M mutual intensity function, which corresponds to a set of M aperture masks that can be shown over time to recreate this desired PSF set. While 3 modes worked well in the example (MSE = $5.4\text{x}10^{-3}$), M can be varied depending upon system specifics to typically (but not always) provide a better estimate for more modes. In this example, 3 modes performs much better than 1 mode, which is used as an example in [1] and offers an MSE=.032.

5. CONCLUSION

Implementing the mode-selection algorithm under a partially coherent framework allows for additional flexibility in the design of depth-dependent PSFs. Future work will consider the tradeoffs involved with optimizing over a different number of modes, an experimental implementation of a dynamic aperture mask, and alternative ways to constrain the decomposition of J to enhance performance.

ACKNOWLEDGMENT

We would like to thank Zhengyun Zhang for helpful discussions and suggestions. This work has been supported in part by a National Defense Science and Engineering Graduate (NDSEG) fellowship awarded through the Air Force Office of Scientific Research. Ramesh Raskar is supported by an Alfred P. Sloan Research Fellowship and a DARPA Young Faculty Award.

REFERENCES

1. Horstmeyer, R., S.B. Oh and R. Raskar, "Iterative aperture mask design in phase space using a rank constraint," *Opt. Express*, Vol. 18, 22545-22555, 2010.
2. Fienup, J. R., "Iterative method applied to image reconstruction and to computer generated holograms," *Opt. Eng.*, Vol. 19, 297–305, 1980.
3. Raymer, M. G., M. Beck and D.F. McAlister, "Complex wave-field reconstruction using phase-space tomography," *Phys. Rev. Lett.* , Vol. 72, No. 8, 1137–1140, 1994.

4. Waller, L., L. Tian and G. Barbastathis, "Transport of Intensity phase-amplitude imaging with higher order intensity derivatives," *Opt. Express* , Vol. 18, 12552–12561, 2010.
5. Brenner, K. H.,A.W. Lohmann and J. Ojeda-Castaneda, "The ambiguity function as a polar display of the OTF," *Opt. Commun.* , Vol. 44, 323–326, 1983.
6. Goodman, J. W., *Introduction to Fourier Optics*, Chap. 6, Mcgraw-Hill, 1982.
7. Ozaktas, H. M.,S. Yuksel and M.A. Kutay, "Linear algebraic theory of partial coherence: discrete fields and measures of partial coherence," *JOSA A* , Vol. 19, No. 8, 1563–1571, 2002.
8. Wolf, E., M., "New theory of partial coherence in the space-frequency domain. Part I: spectra and cross spectra of steady-state sources," *JOSA* , Vol. 72, No. 3, 1982.
9. Hogben, L. M., *Handbook of Linear Algebra* , Chap. 5, Chapman and Hall, New York, 2007.
10. Bastiaans, M., J., "Application of the Wigner distribution function to partially coherent light," *JOSA A* Vol. 3, No. 8, 1227-1238, 1986.
11. DeSantis, P., F. Gori, G. Guattari and C. Palma, "Synthesis of partially coherent fields," *JOSA A*, Vol. 3, No. 8, 1258-1262, 1986.